

Exploring nonequilibrium phases of photo-doped Mott insulators with generalized Gibbs ensembles

Yuta Murakami ^{1✉}, Shintaro Takayoshi², Tatsuya Kaneko³, Zhiyuan Sun ³, Denis Golež ^{4,5}, Andrew J. Millis^{3,6} & Philipp Werner ⁷

Many experiments show that strong excitations of correlated quantum materials can cause non-thermal phases without equilibrium analogues. Understanding the origin and properties of these nonequilibrium states has been challenging due to the limitations of theoretical methods for nonequilibrium strongly correlated systems. In this work, we introduce a generalized Gibbs ensemble description that enables a systematic analysis of the long-time behavior of photo-doped states in Mott insulators based on equilibrium methods. We demonstrate the power of the method by mapping out the nonequilibrium phase diagram of the one-dimensional extended Hubbard model, which features η -pairing and charge density wave phases in a wide photo-doping range. We furthermore clarify that the peculiar kinematics of photo-doped carriers, and the interaction between them, play an essential role in the formation of these non-thermal phases. Our results establish a new path for the systematic analysis of nonequilibrium strongly correlated systems.

¹Department of Physics, Tokyo Institute of Technology, Meguro, Tokyo 152-8551, Japan. ²Department of Physics, Konan University, Kobe 658-8501, Japan. ³Department of Physics, Columbia University, New York 10027, USA. ⁴Jozef Stefan Institute, Jamova 39, SI-1000 Ljubljana, Slovenia. ⁵Faculty of Mathematics and Physics, University of Ljubljana, Jadranska 19, 1000 Ljubljana, Slovenia. ⁶Center for Computational Quantum Physics, Flatiron Institute, New York 10010, USA. ⁷Department of Physics, University of Fribourg, 1700 Fribourg, Switzerland. ✉email: yuta.murakami@phys.titech.ac.jp

Nonequilibrium control of quantum materials is an intriguing prospect with potentially important technological applications^{1–6}. Experiments with various materials and excitation conditions have reported phenomena not observable in equilibrium including nonthermal ordered phases such as superconducting (SC)-like phases^{4,7–9}, charge density waves (CDW)^{10–12} and excitonic condensation¹³. Among various nonequilibrium protocols, photo-doping is a basic and important one, in which a radiation pulse creates electron- and hole-like charge carriers with a long lifetime on the electronic timescale. Due to the nonthermal distribution of the carriers and the cooperative interplay between them, novel nonequilibrium phases can be induced.

The theory of photo-doping has been extensively discussed for semiconductors, where a rich phase diagram including electron-hole plasmas and exciton gases^{14–19} as well as exciton condensation^{20–22} is found. The physical picture is that, after electrons and holes are created, they rapidly relax within the conduction and valence bands, while their recombination occurs on a much longer timescale. Thus, at the single-particle level, the numbers of electrons and holes are separately conserved, so that in the intermediate time regime one has a pseudoequilibrium state that can be described by an effective equilibrium theory with separate chemical potentials for the electrons and holes^{17–19}.

A situation of great current interest is the photo-doping of Mott insulators. In these systems, exotic equilibrium states such as unconventional SC phases emerge upon chemical doping²³, while photo-doping creates novel pseudoparticle excitations not easily represented in a single-particle picture, e.g., doublons and holons in the single-band case. When the Mott gap is large enough, these excitations are long-lived due to the lack of efficient recombination channels^{24–29}. Therefore, as in semiconductors, a fast intraband relaxation results in a long-lived quasi-steady state. Previous studies based on short-time simulations indicated the emergence of enhanced CDW³⁰ or SC correlations^{31–35}, as well as novel spin-orbital orders³⁶. However, unlike in the semiconductor cases, the long-time behavior of photo-doped Mott insulators is not well understood, due to the lack of appropriate theoretical frameworks.

Steady-state formalisms in which explicit heat/particle baths or other dissipative mechanisms are attached to the system have been recently applied^{37–39}. These formalisms, however, require attention to the influence of the baths and dissipations, and the use of explicitly nonequilibrium methods. An alternative approach is a pseudoequilibrium description as in conventional semiconductors. Crucial differences from semiconductors are that the approximately conserved entities are pseudoparticles (local many-body states) not explicitly appearing in the initial Hamiltonian and that the approximate conservation of their number is not manifest in the Hamiltonian but arises from kinematic constraints. Previous work^{37,40–43} introduced the idea of using the Schrieffer-Wolff (SW) transformation to reformulate the problem in a way that explicitly references the approximately conserved quantities and isolates the terms that eventually lead to full equilibration. However, applications of such effective descriptions have been so far limited to small clusters and weak^{40,41,43} or extreme excitation conditions⁴².

In this work, we introduce a generalized Gibbs ensemble (GGE) type description for the effective model obtained from the SW transformation by incorporating different “chemical potentials for pseudoparticles”, i.e., for the many-body local states. This effective equilibrium description allows us to systematically scan the nonequilibrium states in photo-doped Mott insulators for extended systems using established equilibrium methods. We use this approach to identify and study emerging phases in the photo-doped one-dimensional extended Hubbard model. We determine

the nonequilibrium phase diagram, where η -pairing^{33,35,37,42,44} and CDW phases appear in a wide doping range and reveal the corresponding spectral features. The CDW phase is strongly favored in photo-doped systems, compared to the chemically-doped ones, and it is characterized by unbound doublons and holons in contrast to photo-doped semiconductors where electron-hole binding is an important effect. We show that the kinematics of photo-doped doublons/holons, which is qualitatively different from the electron/hole dynamics in conventional semiconductors, plays an essential role and leads to the development of CDW and η -pairing correlations described by squeezed systems without singly occupied sites.

Results

GGE description for photo-doped Mott insulators. The generic formulation of the GGE description is given in Supplementary Note 1. Here we explain the procedure focussing on the extended Hubbard model, whose Hamiltonian is

$$\hat{H} = -t_{\text{hop}} \sum_{\langle i,j \rangle, \sigma} (c_{i,\sigma}^\dagger c_{j,\sigma} + h.c.) + \hat{H}_U + \hat{H}_V, \quad (1)$$

with $\hat{H}_U = U \sum_i (\hat{n}_{i\uparrow} - \frac{1}{2})(\hat{n}_{i\downarrow} - \frac{1}{2})$ the on-site and $\hat{H}_V = V \sum_{\langle i,j \rangle} (\hat{n}_i - 1)(\hat{n}_j - 1)$ the nearest-neighbor interaction. $\hat{c}_{i\sigma}^\dagger$ is the creation operator of a fermion with spin σ at site i , $\hat{n}_{i\sigma} = \hat{c}_{i\sigma}^\dagger \hat{c}_{i\sigma}$ the spin-density at site i , $\hat{n}_i = \hat{n}_{i\uparrow} + \hat{n}_{i\downarrow}$, and $\langle i, j \rangle$ denotes pairs of nearest-neighbor sites. t_{hop} is the hopping parameter. For large U , the half-filled equilibrium system is Mott insulating.

Photo-doping the Mott insulator creates doublons (doubly occupied states) and holons (empty states). When the Mott gap is large, the number of these excited local states is approximately conserved for kinematic reasons^{24–29}. However, the original Hamiltonian explicitly contains recombination terms, which generate virtual processes that affect the physics even when recombination is kinematically suppressed. In order to explicitly remove the recombination terms, while effectively taking account of the effects of virtual recombination processes, we apply the SW transformation^{37,45,46}. Here, we assume $U \gg V, t_{\text{hop}}$. The effective Hamiltonian up to $\mathcal{O}(t_{\text{hop}}^2/U)$ is

$$\hat{H}_{\text{eff}} = \hat{H}_U + \hat{H}_{\text{kin,holon}} + \hat{H}_{\text{kin,doub}} + \hat{H}_V + \hat{H}_{\text{spin,ex}} + \hat{H}_{\text{dh,ex}} + \hat{H}_{U,\text{shift}}^{(2)} + \hat{H}_{3\text{-site}}, \quad (2)$$

where $\hat{H}_{\text{kin,holon}}$ and $\hat{H}_{\text{kin,doub}}$ describe the hopping of holons and doublons of $\mathcal{O}(t_{\text{hop}})$, respectively. The remaining terms are of $\mathcal{O}(t_{\text{hop}}^2/U)$. $\hat{H}_{\text{spin,ex}}$ is the spin-exchange term, $\hat{H}_{\text{dh,ex}}$ is the doublon-holon exchange term and $\hat{H}_{U,\text{shift}}^{(2)}$ describes the shift of the local interaction. $\hat{H}_{3\text{-site}}$ represents three-site terms such as correlated doublon hoppings, see Method. $\hat{H}_{\text{dh,ex}}$ sets the correlations between the neighboring doublons and holons as $\hat{H}_{\text{spin,ex}}$ sets spin correlations between singlons (singly occupied states). In this sense, the above model is a natural extension of the t - J model²³, which is obtained by assuming that either holons or doublons are added (chemical doping) and ignoring $\hat{H}_{3\text{-site}}$.

Due to intraband scattering and environmental coupling (e.g., phonons), intraband relaxation occurs and the system reaches a steady state. Since the numbers of doublons and holons are conserved in the effective model, the steady state can be described by introducing separate “chemical potentials” for them. The corresponding number operators are $\hat{N}_{\text{holon}} = \sum_i \hat{n}_{i,h}$ with $\hat{n}_{i,h} = (1 - \hat{n}_{i\uparrow})(1 - \hat{n}_{i\downarrow})$ and $\hat{N}_{\text{doub}} = \sum_i \hat{n}_{i,d}$ with $\hat{n}_{i,d} = \hat{n}_{i\uparrow} \hat{n}_{i\downarrow}$, respectively. With these, the grand-canonical effective Hamiltonian \hat{K}_{eff}

can be written as $\hat{H}_{\text{eff}} = \mu_{\text{holon}} \hat{N}_{\text{holon}} - \mu_{\text{doubl}} \hat{N}_{\text{doubl}}$, or

$$\hat{K}_{\text{eff}} = \hat{H}_{\text{eff}} - \mu_U \sum_i \hat{n}_{i\uparrow} \hat{n}_{i\downarrow} - \mu \sum_i \hat{n}_i, \quad (3)$$

where $\mu_U = \mu_{\text{doubl}} + \mu_{\text{holon}}$ and $\mu = -\mu_{\text{holon}}$. Thus, the local interaction is modified from U by the photo-doping ($U - \mu_U$), i.e., the energy difference between the doublons and holons is effectively reduced, analogously to the effective shift of the band splitting in photo-doped semiconductors^{22,47}. The properties of the nonequilibrium steady states may then be described by the density matrix $\hat{\rho}_{\text{eff}} = \exp(-\beta_{\text{eff}} \hat{K}_{\text{eff}})$ with an effective temperature $T_{\text{eff}} = 1/\beta_{\text{eff}}$ ^{17,22,48}, which is a sort of GGE^{49,50}. This is essentially an equilibrium problem that can be studied with established equilibrium techniques. Response functions $-i([\hat{A}(t), \hat{B}(0)]_{\pm})$ of the nonequilibrium states can also be computed within this framework, see Supplementary Note 2. Our basic assumption that the nonequilibrium states can be characterized by a few parameters, such as the doublon number and effective temperature, is supported by a recent study³⁷ which demonstrated a good agreement between time-evolving states and nonequilibrium steady states weakly coupled to thermal baths.

Nonequilibrium phase diagram of the photo-doped extended Hubbard model. We apply the above framework to the half-filled one-dimensional extended Hubbard model using infinite time-evolving block decimation (iTEBD)⁵¹ and exact diagonalization (ED)⁵². As in the case of the t - J model, the effect of $\hat{H}_{3\text{-site}}$ is not essential. We confirm this for the photo-doped situation using ED in Supplementary Note 5. Thus, in the following, we focus on the effective model $\hat{H}_{\text{eff}2}$, which ignores $\hat{H}_{3\text{-site}}$. We consider cold systems ($T_{\text{eff}} = 0$) to clarify the possible emergence of nonequilibrium ordered phases. Such a situation may be achieved by energy dissipation to the environment^{47,53,54} or entropy reshuffling^{55,56}. In the following, we use t_{hop} as the energy unit, and fix $U = 10$, i.e., the exchange energy is $J_{\text{ex}} \equiv \frac{4t_{\text{hop}}^2}{U} = 0.4$. We examine the charge correlations $\chi_c(r) \equiv \frac{1}{N} \sum_i (\hat{n}_{i+r} - n_{\text{av}})(\hat{n}_i - n_{\text{av}})$, spin correlations $\chi_s(r) \equiv \frac{1}{N} \sum_i (\hat{s}_{i+r}^z \hat{s}_i^z)$, and SC correlations $\chi_{\text{sc}}(r) \equiv \frac{1}{N} \sum_i (\hat{\Delta}_{i+r} \hat{\Delta}_i)$. Here, N is the system size, $n_{\text{av}} = \frac{1}{N} \sum_i \langle \hat{n}_i \rangle$, $\hat{s}_i^z = \frac{1}{2}(\hat{n}_{i\uparrow} - \hat{n}_{i\downarrow})$, and $\hat{\Delta}_i = \hat{c}_{i\uparrow} \hat{c}_{i\downarrow}$. η -pairing is characterized by staggered SC correlations. Note that \hat{H} , \hat{H}_{eff} , and $\hat{H}_{\text{eff}2}$ are $\text{SU}_c(2)$ symmetric with respect to the η -operators for $V = 0$ ^{44,57}. Due to this symmetry, a homogeneous state with long-range η -SC correlations is on the verge of phase separation, which we avoid by considering nonzero V ⁴², see Supplementary Note 4.

In Fig. 1, we show the computed nonequilibrium phase diagram for the photo-doped Mott insulator in the plane of the doublon density ($n_d = \frac{1}{N} \sum_i \langle \hat{n}_{i,d} \rangle$) and V . In one-dimensional quantum systems, spatial equal-time correlations can show quasi-long-range order, i.e., power-law decay with a critical exponent a less than 2, which corresponds to a diverging susceptibility in the low-frequency limit⁵⁸. The corresponding spatial dependence of the correlation functions is shown on a normal scale in Fig. 2a and on a log scale in Fig. 2b–d. We see that generically more than one correlation function exhibits quasi-long-ranged order. The phase shown in Fig. 1 is identified from the correlation function with the smallest critical exponent. Without photo-doping, an SDW phase with staggered spin correlations is found. However, other correlations quickly become dominant with photo-doping. When $V \lesssim 0.2$ ($= \frac{J_{\text{ex}}}{2}$), the η -SC phase emerges in a wide photo-doping range. This is consistent with recent dynamical mean-field theory (DMFT) analyses for the pure Hubbard model in infinite spatial dimensions employing entropy cooling or heat baths^{37,55}. Importantly, the sign of the SC correlations remains staggered

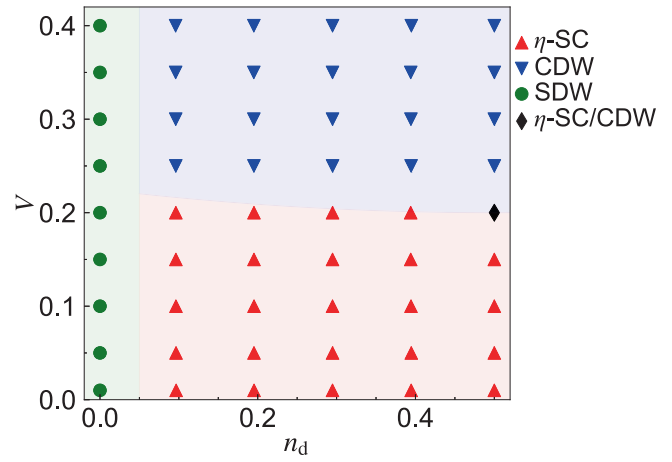


Fig. 1 Nonequilibrium phase diagram of the half-filled photo-doped Mott insulator. The nonequilibrium phase diagram described by the effective Hamiltonian $\hat{H}_{\text{eff}2}$ is shown in the plane of the doublon density (n_d) and the nonlocal interaction V , for the local Coulomb interaction $U = 10$. It includes the η -pairing (η -SC) phase, the charge density wave (CDW) phase and the spin-density wave (SDW) phase. The phases are categorized by the dominant correlation evaluated from the infinite time-evolving block decimation, i.e., the correlation with the smallest critical exponent a . The critical exponent is extracted by fitting the correlation functions ($\chi(r)$) with $C_1/r^2 + C_2 \cos(qr)/r^a$, where $q = 2n_d\pi$, $q = (1 - 2n_d)\pi$, and $q = \pi$ for charge, spin, and SC correlations, respectively. We use the spatial distance $r \in [6, 30]$ for the fitting range. The phase boundary is only schematic and a guide to the eye except for $n_d = 0.5$ and $V = J_{\text{ex}}/2$, where η -SC and CDW are degenerated (η -SC/CDW).

regardless of doping and V . For larger V , the CDW phase is stabilized. We note that, in the extreme photo-doping limit ($n_d = 0.5$), the effective model ($\hat{H}_{\text{dh,ex}} + \hat{H}_V$) becomes equivalent to the XXZ model⁴². Namely, we have

$$\hat{H}_{\text{eff}} = J_{\text{XY}} \sum_{\langle i,j \rangle} [\hat{\eta}_i^x \hat{\eta}_j^x + \hat{\eta}_i^y \hat{\eta}_j^y] + J_Z \sum_{\langle i,j \rangle} \hat{\eta}_i^z \hat{\eta}_j^z, \quad (4)$$

where $J_{\text{XY}} = -J_{\text{ex}}$, $J_Z = -J_{\text{ex}} + 4V$ and $\hat{\eta}$ represents the η -operators (see Methods). The XXZ model shows XY order (quasi-long-range order) for $|J_{\text{XY}}| > J_Z$, while it shows Ising order (long-range order) for $|J_{\text{XY}}| < J_Z$. In our language, the former corresponds to η -SC and the latter to CDW. Thus, it is natural that the phase transition between η -SC and CDW occurs at $|J_{\text{XY}}| = J_Z$, i.e., $V = \frac{J_{\text{ex}}}{2}$, for strong photo-doping. Interestingly, the phase boundary remains located near this value over a wide photo-doping range, see Fig. 1.

As Fig. 2b–d shows, more than one order can be quasi-long ranged for a given set of parameters. When V is small, the SC correlations are dominant. The spin correlations are also quasi-long-ranged, while the charge correlations show no sign of CDW (alternation of signs). When V is increased, the exponent of the spin correlations remains almost unchanged, while the decay of the SC correlations becomes faster, and the CDW correlation starts to develop around $V \gtrsim 0.1$ ($= \frac{J_{\text{ex}}}{4}$). $V = 0.2$ ($= \frac{J_{\text{ex}}}{2}$) is in a coexistence regime where CDW, SDW, and η -SC orders are simultaneously quasi-long ranged. While the precise boundaries of the coexistence regime are difficult to determine (see Supplementary Note 3), by $V = 0.4$ ($= J_{\text{ex}}$), the CDW correlations become dominant and the SC correlations decay exponentially.

Origin and properties of the photo-doped phases. The photo-doped states exhibit unique properties. Firstly, the η -SC is absent in equilibrium, since in chemically-doped systems either

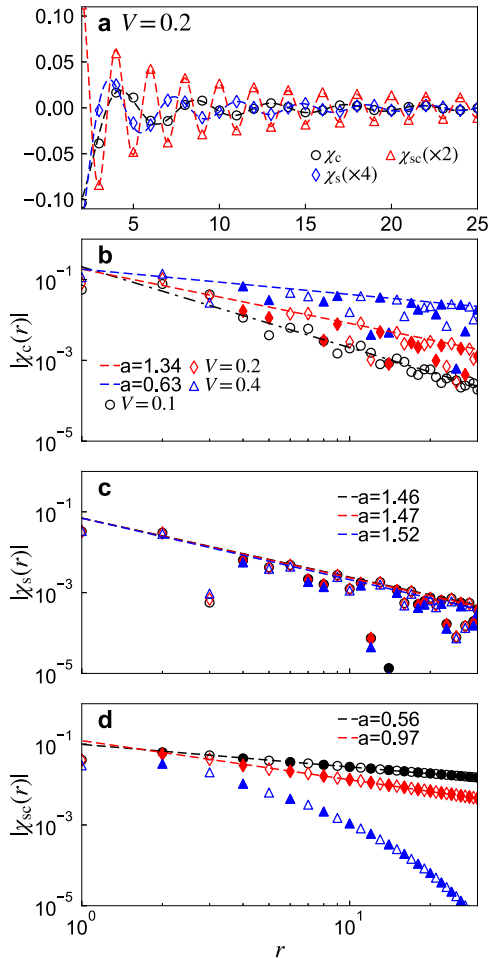


Fig. 2 Correlation functions of the photo-doped states. Correlation functions for charge (χ_c), spin (χ_s), and superconductivity (χ_{sc}) are evaluated with the infinite time-evolving block decimation for the photo-doped states described by the effective Hamiltonian \hat{H}_{eff2} . **a** Normal scale plot for the nonlocal interaction $V = 0.2$ and the corresponding fitting with $C_1/r^2 + C_2 \cos(qr)/r^a$, where $q = 2n_d\pi$, $q = (1 - 2n_d)\pi$, and $q = \pi$ for charge, spin and SC correlations, respectively. Here, r is the spatial distance, n_d is the doublon density, and C_1 , C_2 , and the critical exponent a are fitting parameters. **b-d** Log-scale plots of the absolute value of the correlation functions for specified values of V . Empty (filled) markers correspond to $\chi < 0$ ($\chi > 0$). The dashed (dot-dashed) lines show $C_2 r^{-a}$ ($C_1 r^{-2}$) extracted by fitting. For all panels, we use $n_d = 0.23$ and $r \in [6, 30]$ for the fitting range.

doublons or holons are introduced and hence $\chi_{sc}(r)$ vanishes. On the other hand, one expects that even in chemically-doped states, CDWs can develop due to the instability of the Fermi surface. Figure 3a, b however show that the CDW correlations are much stronger in photo-doped than in chemically-doped states. Furthermore, the CDW correlations show incommensurate oscillations with $q = 2n_d\pi$, see Fig. 2a. This indicates that holons and doublons do not bind in pairs. Instead, the holons (doublons) are located in the middle of neighboring doublons (holons), even though the doublon-holon interaction $V_{dh} \equiv \frac{J_{ex}}{4} - V$ is attractive, see $\hat{H}_{dh,ex} + \hat{H}_V$. The absence of binding is also directly confirmed by the evaluation of the doublon-holon correlations (Supplementary Note 2). This situation is in stark contrast with semiconductors, where the attractive interaction between photo-doped holes and electrons leads to condensation of electron-hole pairs (excitons) at low temperatures^{20–22,47}.

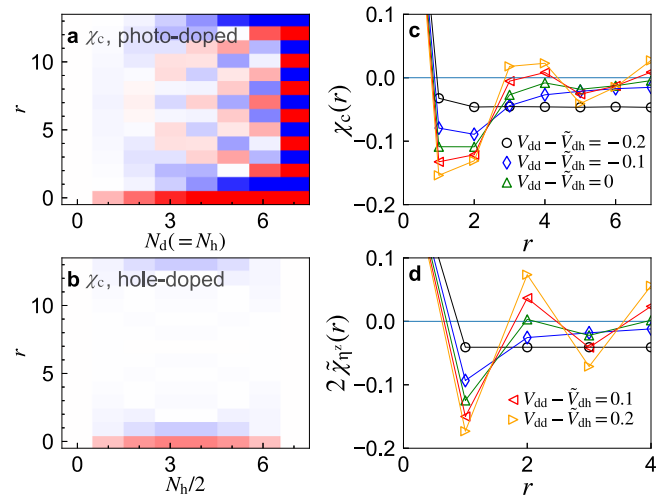


Fig. 3 Characteristic features of the photo-induced charge density wave phase. **a, b** Charge correlation function $\chi_c(r)$ for the photo-doped and hole-doped states described by the effective Hamiltonian \hat{H}_{eff2} . Here $N_{d(h)}$ indicates the number of doublons (holons). **c, d** Dependence of $\chi_c(r)$ (**c**) and the charge correlation function in the squeezed space $\tilde{\chi}_{\eta}(r)$ (**d**) on the relative magnitude of V_{dd} and \tilde{V}_{dh} for states described by the effective model $\hat{H}_{\text{eff2}} + \hat{H}_{V_{dh}}$. Here V_{dd} is the interaction between doublons (and between holons) and \tilde{V}_{dh} is the interaction between a doublon and a holon. In all panels, we set the system size $N = 14$ and the nonlocal interaction $V = 0.4$, and use the exact diagonalization method. In **c** and **d**, we set $N_d = N_h = 4$.

Let us discuss in more detail the physical origin of the CDW phase. In the extended Hubbard model the interaction between doublons (and between holons) is $V_{dd} \equiv -\frac{J_{ex}}{4} + V$, and thus $V_{dd} = -V_{dh}$. To investigate how the interactions among doublons and holons affect the CDW formation, we artificially add an interaction between neighboring doublons and holons, $\hat{H}_{V_{dh}} \equiv \Delta V_{dh} \sum_i [\hat{n}_{i,d} \hat{n}_{i+1,h} + \hat{n}_{i,h} \hat{n}_{i+1,d}]$, so that the doublon-holon interaction becomes $\tilde{V}_{dh} \equiv V_{dh} + \Delta V_{dh}$. We choose parameters such that both \tilde{V}_{dh} and V_{dd} are repulsive. Figure 3c shows that the relative magnitude of the doublon-doublon (holon-holon) and doublon-holon interaction controls the physics and that an attractive doublon-holon interaction is not essential for the CDW. Namely, oscillations in χ_c appear if $V_{dd} \gtrsim \tilde{V}_{dh}$. This indicates that CDW correlations develop between the doublons and holons as if no singlons existed between them. The situation is analogous to the spin correlations in the one-dimensional t - J model, which can be explained by the squeezed Heisenberg chain without doublons and holons^{59,60}. Underlying this phenomenon in the one-dimensional t - J model is the conservation of the spin configuration in the $J \rightarrow 0$ limit⁵⁹. Since a singlon always encounters the same neighbors, the system favors the spin configurations described by the Heisenberg hamiltonian. The same situation is realized in the photo-doped case. In the limit of $J_{ex} \rightarrow 0$, the configuration of doublons and holons is also conserved due to their peculiar kinematics, see $\hat{H}_{\text{kin,holon}} + \hat{H}_{\text{kin,doub}}$. (Note that in normal semiconductors, holes and electrons can switch positions even in the one-dimensional case.) Thus, the configurations of doublons and holons are determined by the interaction term $\hat{H}_{dh,ex} + \hat{H}_V$, as in the case of spin configurations in the t - J model.

To confirm the above scenario, we evaluate the correlations between the doublons and holons in terms of a reduced distance which ignores singlons. The corresponding correlation function is defined as $\tilde{\chi}_{\eta_z}(r) = \langle \sum_{l \geq 0} Q_l \hat{\eta}_{r+l}^z \hat{\eta}_0^z Q_l \rangle$ ⁴¹, where Q_l is the

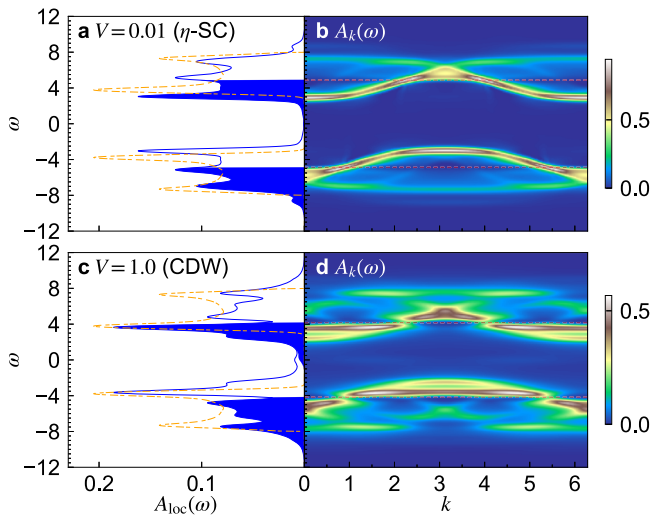


Fig. 4 Single-particle spectral functions for the η -pairing (η -SC) phase and the charge density wave (CDW) phase. The momentum-integrated spectrum $A_{\text{loc}}(\omega)$ and the momentum-resolved spectrum $A_k(\omega)$ for the photo-doped states described by the effective Hamiltonian \hat{H}_{eff2} are evaluated with the infinite time-evolving block decimation. **a** and **b** are for the η -SC phase, while **c** and **d** are for the CDW phase. In **a** and **c**, the filled regions indicate the occupied states and dot-dashed lines show $A_{\text{loc}}(\omega)$ for the equilibrium (non-photo-doped) states. In **b** and **d**, dashed lines indicate the Fermi levels in the UHB and LHB. Here, the doublon density is $n_d = 0.23$.

projection to states with l singlons between the 0th site and the $(r + l)$ th site and $\hat{n}_i^z = \frac{1}{2}(\hat{n}_{i,d} - \hat{n}_{i,h})$ [Fig. 3d]. Staggered correlations appear for $V_{dd} \gtrsim \tilde{V}_{dh}$, which supports the above argument. Note that, even when doublons and holons show Ising-type order in the squeezed space, the correlations can still exhibit a power-law⁶¹. We thus conclude that the photo-induced CDW originates from the less repulsive doublon–holon interaction (compared to interactions between the same species), the peculiar kinematics of carriers and the one-dimensional configuration. Furthermore, the development of correlations between the doublons and holons in the squeezed system without singlons should also apply to systems with $V \lesssim \frac{J_{\text{ex}}}{2}$. In these cases, the X and Y components of $\hat{H}_{\text{dh,ex}} + \hat{H}_V$ (we regard $\hat{H}_{\text{dh,ex}} + \hat{H}_V$ as an XXZ model, as in the extreme photo-doping limit) is dominant and the η -pairing phase emerges. This naturally explains the observation that the boundary between the η -pairing phase and the CDW phase is close to $V \simeq \frac{J_{\text{ex}}}{2}$ independent of the photo-doping level.

Single-particle spectra. We now focus on the single-particle spectra, to clarify characteristic features of the different phases. Figure 4 shows the momentum-integrated spectrum $A_{\text{loc}}(\omega)$ and the momentum-resolved spectrum $A_k(\omega)$ for the η -SC phase [Fig. 4a, b] and the CDW phase [Fig. 4c, d]⁴⁶. For the CDW phase, we use $V = 1$ to enhance the characteristic features. Unlike in equilibrium, but similar to photo-doped semiconductors, the photo-doped system exhibits two “Fermi levels” separating occupied (electron removal spectrum) from unoccupied (electron addition spectrum) states [Fig. 4a, c]. The occupied states in the upper Hubbard band (UHB) region correspond to the removal of a doublon already existing in the photo-doped state, while those in the lower Hubbard band (LHB) region correspond to adding a holon (see Methods for precise definitions). In the η -SC phase, within our numerical accuracy, no gap signature appears in $A_k(\omega)$ around the new Fermi levels [Fig. 4b], which is in stark contrast to a normal

superconductor with a gap around the Fermi level. The absence of a gap is also found for η -pairing states in higher dimensions⁶², and this suggests that the η -SC state is a kind of gapless superconductivity. On the other hand, in the CDW phase, gaps appear at the new Fermi levels [Fig. 4d], as in the excitonic phase in photo-doped semiconductors²².

Finally, we observe that in-gap states between the UHB and LHB develop with photo-doping, which are more prominent for larger V [Fig. 4c]. These states may enable recombination processes suggesting that our assumption of approximately conserved doublon and holon numbers may become less valid as the excitation density increases. However, one needs to keep in mind the following points: (i) For large enough U , the Mott gap remains clear and the doublon and holon numbers are approximately conserved. Since the CDW is driven by V , the value of U does not affect its existence and spectral features. (ii) Even when in-gap states develop, an effective equilibrium description is meaningful. The recombination rate for a given state can be estimated by Fermi’s golden rule, and if this rate is small compared to the intraband relaxation, the transient state can be described by (time-dependent) effective temperatures and chemical potentials⁶³. Hence, our results show that the effective equilibrium description can be useful to study the closure or shrinking of a Mott gap via photo-doping, as a result of screened interactions and photo-induced spectral features⁶⁴.

Discussion

We introduced a GGE-type effective equilibrium description for photo-doped strongly correlated systems. This provides a theoretical framework for systematic studies of nonthermal phases. Using this effective equilibrium description, we revealed emerging phases in the photo-doped one-dimensional extended Hubbard model. The η -pairing phase is stabilized in the small V regime even when the $SU_c(2)$ symmetry that protects η -pairing in the pure Hubbard model is absent, and it is characterized by gapless spectra. The CDW phase emerges in the larger V regime, and it is characterized by gapped spectra. These states are unique to a photo-doped strongly correlated system, where the peculiar kinematics of doublons and holons stabilizes them in a wide doping range. The similarity between the GGE-type description for strongly correlated systems and the pseudoequilibrium description for the photo-doped semiconductors allowed us to clarify some fundamental differences between these two systems. In particular, our results demonstrate that photo-doped strongly correlated systems and semiconductors exhibit qualitatively different phases due to the different nature of the injected carriers. Target systems to look for the characteristic Mott features include candidate materials of one-dimensional Mott insulators ranging from organic crystals, e.g., ET-F₂TCNQ, to cuprates, e.g., Sr₂CuO₃, as well as cold-atom systems.

We also note that further insights into our results may be obtained by using equilibrium concepts such as Luttinger liquid theory and the exact wave function for $J_{\text{ex}} \rightarrow 0$ ⁵⁹. In the nonequilibrium state, we expect at most three degrees of freedom: spin, pseudo-spin (consisting of doublon and holon), and charge (position of singlons). Thus, unlike in the equilibrium case, the maximum value of the conformal charge c would be 3, which may be realized in the η -pairing phase. A systematic analysis in this direction is under consideration.

The GGE-type description of photo-doped Mott states can be applied to various models and implemented with different equilibrium techniques such as slave boson approaches^{65,66} and variational methods^{51,67,68}. It can provide useful insights into experimental findings, e.g., photo-induced SC-like state, as well as theoretical results. For example, a recently found metastable orbital

order in a photo-doped multi-orbital system can be reasonably explained by an effective equilibrium picture⁶⁹. Systematic explorations of nonequilibrium phases in higher dimensions and at nonzero effective temperatures with the GGE-type description should be undertaken. For example, the GGE-type description allows us to investigate important aspects of nonequilibrium states, such as the screening of the interactions⁶⁴ or the stability of photo-induced phases against light irradiation⁷⁰. These questions are interesting topics for future investigation.

Methods

Infinite time-evolving block decimation. The infinite time-evolving block decimation (iTEBD) method expresses the wave function of the system as a matrix product state (MPS), assuming translational invariance⁵¹. iTEBD directly treats the thermodynamic limit and we use cut-off dimensions $D = 1000\text{--}3000$ for the MPS to get converged results. We use the conservation laws for the numbers of spin-up and spin-down electrons at half-filling to improve the efficiency of the calculations. Away from half-filling, the trick with the conservation laws cannot be used, which makes the simulations less efficient. Thus, we use the exact diagonalization method in Fig. 3.

We also note that, to fit correlation functions obtained from iTEBD, we use functions with a power law. To be strict, because of the SU(2) spin symmetry, there may be a logarithmic correction on top of the power-law decay for the spin correlation. Still, in our results, fits with and without this correction work equally well. The latter fit yields larger a , hence the phase diagram and the qualitative arguments given in the main text remain unaffected.

Single-particle spectrum. The single-particle spectrum is defined as follows. The local spectrum is $A_{\text{loc}}(\omega) \equiv -\frac{1}{\pi} \text{Im}G_{\text{loc}}^R(\omega)$ and the momentum-resolved spectrum is $A_k(\omega) \equiv -\frac{1}{\pi} \text{Im}G_k^R(\omega)$. Here, $G_k^R(\omega)$ ($G_k^A(\omega)$) is the Fourier transform of the retarded Green's function $G_k^R(t) = -i\langle[\hat{c}_{k\sigma}(t), \hat{c}_{k\sigma}^\dagger(0)]_+\rangle$ ($G_k^A(t) = -i\langle[\hat{c}_{k\sigma}(t), \hat{c}_{k\sigma}^\dagger(0)]_+\rangle$). Note that $\hat{c}_{i\sigma}(t)$ is the Heisenberg representation of \hat{c} in terms of \hat{H}_{eff} . The occupied spectra correspond to $A_{\text{loc}}^<(\omega) \equiv \frac{1}{2\pi} \text{Im}G_{\text{loc}}^<(\omega)$ and $A_k^<(\omega) \equiv \frac{1}{2\pi} \text{Im}G_k^<(\omega)$, where $G^<$ denotes the lesser part of the Green's functions. To evaluate these quantities using the effective equilibrium description and iTEBD, we employ the method proposed by some of the authors⁴⁶. Namely, we evaluate $G^R(t)$ using an auxiliary band and perform the Fourier transformation with a Gaussian window, $F_{\text{Gauss}}(t) = \exp(-\frac{t^2}{2\sigma^2})$, and we use $\sigma = 5.0$. Thus, the broadening of the resultant spectrum is inevitable and a gap much smaller than the broadening cannot be captured. Still, we checked that no gap signature appears in the η pairing state for an increased value of J_{ex} , where we would expect an increase of the gap (if any).

H_{eff} for the U-V Hubbard model. The explicit expressions for the terms in Eq. (2) are as follows. The $\mathcal{O}(t_{\text{hop}})$ terms are given by

$$\hat{H}_{\text{kin,holon}}(t) = -t_{\text{hop}} \sum_{(i,j),\sigma} \bar{n}_{i,\bar{\sigma}} (\hat{c}_{i,\sigma}^\dagger \hat{c}_{j,\sigma} + h.c.) \bar{n}_{j,\bar{\sigma}}, \quad (5)$$

$$\hat{H}_{\text{kin,doublon}}(t) = -t_{\text{hop}} \sum_{(i,j),\sigma} n_{i,\bar{\sigma}} (\hat{c}_{i,\sigma}^\dagger \hat{c}_{j,\sigma} + h.c.) n_{j,\bar{\sigma}}, \quad (6)$$

where $\bar{n} = 1 - n$ and $\bar{\sigma}$ is the opposite spin to σ .

For the $\mathcal{O}(\frac{t_{\text{hop}}^2}{U})$ terms, we introduce the exchange coupling $J_{\text{ex}} = \frac{4t_{\text{hop}}^2}{U}$. With this, the spin-exchange term becomes

$$\hat{H}_{\text{spin,ex}} = J_{\text{ex}} \sum_{(i,j)} \hat{s}_i \cdot \hat{s}_j, \quad (7)$$

where $\hat{s} = \frac{1}{2} \hat{c}_\alpha^\dagger \sigma_{\alpha\beta} \hat{c}_\beta$ with σ denoting the Pauli matrices. The exchange term for a doublon and a holon on neighboring sites is

$$\hat{H}_{\text{dh,ex}} = -J_{\text{ex}} \sum_{(i,j)} [\hat{\eta}_i^x \hat{\eta}_j^x + \hat{\eta}_i^y \hat{\eta}_j^y + \hat{\eta}_i^z \hat{\eta}_j^z]. \quad (8)$$

Here, we introduce the η -operators as $\hat{\eta}_i^+ = \theta_i \hat{c}_{i1}^\dagger \hat{c}_{i1}^\dagger$, $\hat{\eta}_i^- = \theta_i \hat{c}_{i1} \hat{c}_{i1}$ and $\hat{\eta}_i^z = \frac{1}{2}(\hat{n}_i - 1)$ with $\theta_i = (-)^i$. The shift of the local interaction is described by

$$\hat{H}_{U,\text{shift}}^{(2)} = J_{\text{ex}} \sum_i \left(\hat{n}_{i1} - \frac{1}{2} \right) \left(\hat{n}_{i1} - \frac{1}{2} \right). \quad (9)$$

Here, the superscript “(2)” indicates that the term is order of $\mathcal{O}(\frac{t_{\text{hop}}^2}{U})$.

The three-site term can be expressed as $\hat{H}_{3\text{-site}} \equiv \hat{H}_{\text{kin,holon}}^{(2)} + \hat{H}_{\text{kin,doub}}^{(2)} + \hat{H}_{\text{dh,slide}}^{(2)}$. Here, $\hat{H}_{\text{kin,holon}}^{(2)}$ and $\hat{H}_{\text{kin,doub}}^{(2)}$ are correlated hoppings of holons and doublons, while

$\hat{H}_{\text{dh,slide}}^{(2)}$ shifts the position of a doublon and a holon. Their expressions are

$$\hat{H}_{\text{kin,holon}}^{(2)} = \frac{J_{\text{ex}}}{4} \sum_{(k,i,j),\sigma} \left[n_{i,\bar{\sigma}} \hat{c}_{j,\sigma} \bar{n}_{j,\bar{\sigma}} \bar{n}_{k,\sigma} \hat{c}_{k,\sigma}^\dagger + h.c. \right] - \frac{J_{\text{ex}}}{4} \sum_{(k,i,j),\sigma} \left[\bar{n}_{k,\sigma} \hat{c}_{k,\sigma}^\dagger \hat{c}_{i,\bar{\sigma}} \hat{c}_{j,\sigma} \bar{n}_{j,\bar{\sigma}} + h.c. \right], \quad (10)$$

$$\hat{H}_{\text{kin,doublon}}^{(2)} = \frac{J_{\text{ex}}}{4} \sum_{(k,i,j),\sigma} \left[\bar{n}_{i,\bar{\sigma}} \hat{c}_{j,\sigma}^\dagger n_{j,\bar{\sigma}} n_{k,\bar{\sigma}} \hat{c}_{k,\sigma} + h.c. \right] - \frac{J_{\text{ex}}}{4} \sum_{(k,i,j),\sigma} \left[\hat{c}_{i,\bar{\sigma}}^\dagger n_{k,\sigma} \hat{c}_{k,\sigma} n_{j,\bar{\sigma}} \hat{c}_{j,\sigma}^\dagger \hat{c}_{i,\sigma} + h.c. \right], \quad (11)$$

and

$$\hat{H}_{\text{dh,slide}}^{(2)} = \frac{J_{\text{ex}}}{4} \sum_{(k,i,j),\sigma} \left[\hat{c}_{i\sigma}^\dagger \hat{c}_{j,\sigma} \bar{n}_{j,\bar{\sigma}} \hat{c}_{i,\bar{\sigma}} \hat{c}_{k,\sigma} n_{k,\sigma} + h.c. \right] + \frac{J_{\text{ex}}}{4} \sum_{(k,i,j),\sigma} \left[n_{j,\bar{\sigma}} \hat{c}_{j,\sigma}^\dagger n_{k,\sigma} \bar{n}_{k,\bar{\sigma}} \hat{c}_{k,\sigma}^\dagger \hat{c}_{i,\sigma} + h.c. \right]. \quad (12)$$

Here, $\langle k, i, j \rangle$ means that both of (k, i) and (i, j) are pairs of neighboring sites. The sum is over all possible such combinations (without double counting), where we regard $\langle k, i, j \rangle = \langle j, i, k \rangle$.

In the evaluation of the physical quantities, we use the operators of the effective model. To be strict, if physical quantities for the original Hamiltonian are to be computed, one also needs to take account of corrections from the SW transformation to the operators. However, these corrections are not necessary to see the leading behavior. The same strategy is often used in the evaluation of physical quantities for the Heisenberg model or the t - J model.

Data availability

The data that support the findings of this study are available from the corresponding author upon reasonable request.

Code availability

The source code for the calculations performed in this work is available from the corresponding authors upon reasonable request.

Received: 2 August 2021; Accepted: 22 December 2021;

Published online: 13 January 2022

References

- Yonemitsu, K. & Nasu, K. Theory of photoinduced phase transitions in itinerant electron systems. *Phys. Rep.* **465**, 1–60 (2008).
- Giannetti, C. et al. Ultrafast optical spectroscopy of strongly correlated materials and high-temperature superconductors: a non-equilibrium approach. *Adv. Phys.* **65**, 58–238 (2016).
- Basov, D. N., Averitt, R. D. & Hsieh, D. Towards properties on demand in quantum materials. *Nat. Mater.* **16**, 1077–1088 (2017).
- Cavalleri, A. Photo-induced superconductivity. *Contemp. Phys.* **59**, 31–46 (2018).
- Oka, T. & Kitamura, S. Floquet engineering of quantum materials. *Annu. Rev. Condens. Matter Phys.* **10**, 387–408 (2019).
- de la Torre, A. et al. Nonthermal pathways to ultrafast control in quantum materials <https://journals.aps.org/rmp/abstract/10.1103/RevModPhys.93.041002> (2021).
- Fausti, D. et al. Light-induced superconductivity in a stripe-ordered cuprate. *Science* **331**, 189–191 (2011).
- Mitrano, M. et al. Possible light-induced superconductivity in K_3C_{60} at high temperature. *Nature* **530**, 461–464 (2016). Letter.
- Suzuki, T. et al. Photoinduced possible superconducting state with long-lived disproportionate band filling in FeSe. *Commun. Phys.* **2**, 115 (2019).
- Stojchevska, L. et al. Ultrafast switching to a stable hidden quantum state in an electronic crystal. *Science* **344**, 177–180 (2014).
- Matsuzaki, H. et al. Excitation-photon-energy selectivity of photoconversions in halogen-bridged pd-chain compounds: Mott insulator to metal or charge-density-wave state. *Phys. Rev. Lett.* **113**, 096403 (2014).
- Kogar, A. et al. Light-induced charge density wave in LaTe_3 . *Nat. Phys.* **16**, 159–163 (2020).
- Murotani, Y. et al. Light-driven electron-hole Bardeen-Cooper-Schrieffer-like state in bulk GaAs. *Phys. Rev. Lett.* **123**, 197401 (2019).
- Mott, N. F. The transition to the metallic state. *Philos. Mag.* **6**, 287–309 (1961).

15. Schmitt-Rink, S., Löwenau, J. & Haug, H. Theory of absorption and refraction of direct-gap semiconductors with arbitrary free-carrier concentrations. *Z. Phys. B* **47**, 13–17 (1982).
16. Zimmermann, R. & Stolz, H. The mass action law in two-component fermi systems revisited excitons and electron-hole pairs. *Phys. Status Solidi (B)* **131**, 151–164 (1985).
17. Haug, H. & Koch, S. W. *Quantum Theory of the Optical and Electronic Properties of Semiconductors* (World Scientific, 1990).
18. Keldysh, L. V. The electron-hole liquid in semiconductors. *Contemp. Phys.* **27**, 395–428 (1986).
19. Asano, K. & Yoshioka, T. Exciton-mott physics in two-dimensional electron-hole systems: phase diagram and single-particle spectra. *J. Phys. Soc. Jpn.* **83**, 084702 (2014).
20. Keldish, L. V. & Kopaev, Y. V. Possible instability of the semimetallic state toward Coulomb interaction. *Sov. Phys. Solid State* **6**, 2219 (1965).
21. Jérôme, D., Rice, T. M. & Kohn, W. Excitonic insulator. *Phys. Rev.* **158**, 462–475 (1967).
22. Peretto, E., Sangalli, D., Marini, A. & Stefanucci, G. Pump-driven normal-to-excitonic insulator transition: Josephson oscillations and signatures of bec-bcs crossover in time-resolved arpes. *Phys. Rev. Mater.* **3**, 124601 (2019).
23. Imada, M., Fujimori, A. & Tokura, Y. Metal-insulator transitions. *Rev. Mod. Phys.* **70**, 1039–1263 (1998).
24. Strohmaier, N. et al. Observation of elastic doublon decay in the fermi-hubbard model. *Phys. Rev. Lett.* **104**, 080401 (2010).
25. Lenarčič, Z. & Prelovšek, P. Ultrafast charge recombination in a photoexcited mott-hubbard insulator. *Phys. Rev. Lett.* **111**, 016401 (2013).
26. Mitrano, M. et al. Pressure-dependent relaxation in the photoexcited mott insulator ET – f_2 TCNQ: influence of hopping and correlations on quasiparticle recombination rates. *Phys. Rev. Lett.* **112**, 117801 (2014).
27. Sensarma, R. et al. Lifetime of double occupancies in the fermi-hubbard model. *Phys. Rev. B* **82**, 224302 (2010).
28. Eckstein, M. & Werner, P. Thermalization of a pump-excited mott insulator. *Phys. Rev. B* **84**, 035122 (2011).
29. Lenarčič, Z. & Prelovšek, P. Charge recombination in undoped cuprates. *Phys. Rev. B* **90**, 235136 (2014).
30. Lu, H., Sota, S., Matsueda, H., Bonča, J. & Tohyama, T. Enhanced charge order in a photoexcited one-dimensional strongly correlated system. *Phys. Rev. Lett.* **109**, 197401 (2012).
31. Wang, Y., Chen, C.-C., Moritz, B. & Devereaux, T. P. Light-enhanced spin fluctuations and d -wave superconductivity at a phase boundary. *Phys. Rev. Lett.* **120**, 246402 (2018).
32. Bittner, N., Tohyama, T., Kaiser, S. & Manske, D. Possible light-induced superconductivity in a strongly correlated electron system. *J. Phys. Soc. Jpn.* **88**, 044704 (2019).
33. Kaneko, T., Shirakawa, T., Sorella, S. & Yunoki, S. Photoinduced η pairing in the hubbard model. *Phys. Rev. Lett.* **122**, 077002 (2019).
34. Kaneko, T., Yunoki, S. & Millis, A. J. Charge stiffness and long-range correlation in the optically induced η -pairing state of the one-dimensional hubbard model. *Phys. Rev. Res.* **2**, 032027 (2020).
35. Ejima, S., Kaneko, T., Lange, F., Yunoki, S. & Fehske, H. Photoinduced η -pairing at finite temperatures. *Phys. Rev. Res.* **2**, 032008 (2020).
36. Li, J., Strand, H. U. R., Werner, P. & Eckstein, M. Theory of photoinduced ultrafast switching to a spin-orbital ordered hidden phase. *Nat. Commun.* **9**, 4581 (2018).
37. Li, J., Golež, D., Werner, P. & Eckstein, M. η -paired superconducting hidden phase in photodoped mott insulators. *Phys. Rev. B* **102**, 165136 (2020).
38. Li, J. & Eckstein, M. Nonequilibrium steady-state theory of photodoped mott insulators. *Phys. Rev. B* **103**, 045133 (2021).
39. Tindall, J., Buča, B., Coulthard, J. R. & Jaksch, D. Heating-induced long-range η pairing in the hubbard model. *Phys. Rev. Lett.* **123**, 030603 (2019).
40. Takahashi, A., Gomi, H. & Aihara, M. Photoinduced superconducting states in strongly correlated electron systems. *Phys. Rev. B* **66**, 115103 (2002).
41. Gomi, H., Takahashi, A., Ueda, T., Itoh, H. & Aihara, M. Photogenerated holon-doublon cluster states in strongly correlated low-dimensional electron systems. *Phys. Rev. B* **71**, 045129 (2005).
42. Rosch, A., Rasch, D., Binz, B. & Vojta, M. Metastable superfluidity of repulsive fermionic atoms in optical lattices. *Phys. Rev. Lett.* **101**, 265301 (2008).
43. Kanamori, Y., Matsueda, H. & Ishihara, S. Photoinduced change in the spin state of itinerant correlated electron systems. *Phys. Rev. Lett.* **107**, 167403 (2011).
44. Yang, C. N. η pairing and off-diagonal long-range order in a hubbard model. *Phys. Rev. Lett.* **63**, 2144–2147 (1989).
45. Schrieffer, J. R. & Wolff, P. A. Relation between the anderson and kondo hamiltonians. *Phys. Rev.* **149**, 491–492 (1966).
46. Murakami, Y., Takayoshi, S., Koga, A. & Werner, P. High-harmonic generation in one-dimensional mott insulators. *Phys. Rev. B* **103**, 035110 (2021).
47. Murakami, Y., Schüler, M., Takayoshi, S. & Werner, P. Ultrafast nonequilibrium evolution of excitonic modes in semiconductors. *Phys. Rev. B* **101**, 035203 (2020).
48. Yoshioka, T. & Asano, K. Exciton-mott physics in a quasi-one-dimensional electron-hole system. *Phys. Rev. Lett.* **107**, 256403 (2011).
49. Vidmar, L. & Rigol, M. Generalized Gibbs ensemble in integrable lattice models. *J. Stat. Mech.* **06**, 064007 (2016).
50. Lange, F., Lenarčič, Z. & Rosch, A. Pumping approximately integrable systems. *Nat. Commun.* **8**, 15767 (2017).
51. Vidal, G. Efficient classical simulation of slightly entangled quantum computations. *Phys. Rev. Lett.* **91**, 147902 (2003).
52. Dagotto, E. Correlated electrons in high-temperature superconductors. *Rev. Mod. Phys.* **66**, 763–840 (1994).
53. Eckstein, M. & Werner, P. Photoinduced states in a mott insulator. *Phys. Rev. Lett.* **110**, 126401 (2013).
54. Sentef, M. et al. Examining electron-boson coupling using time-resolved spectroscopy. *Phys. Rev. X* **3**, 041033 (2013).
55. Werner, P., Li, J., Golež, D. & Eckstein, M. Entropy-cooled nonequilibrium states of the hubbard model. *Phys. Rev. B* **100**, 155130 (2019).
56. Werner, P., Eckstein, M., Müller, M. & Refael, G. Light-induced evaporative cooling of holes in the hubbard model. *Nat. Commun.* **10**, 5556 (2019).
57. Essler, F. H. L., Frahm, H., Göhmann, F., Klümper, A. & Korepin, V. E. *The One-Dimensional Hubbard Model* (Cambridge Univ. Press, 2005).
58. Giamarchi, T. *Quantum Physics in One Dimension* (Oxford Univ. Press, 2003).
59. Ogata, M. & Shiba, H. Bethe-ansatz wave function, momentum distribution, and spin correlation in the one-dimensional strongly correlated hubbard model. *Phys. Rev. B* **41**, 2326–2338 (1990).
60. Feng, S., Su, Z. B. & Yu, L. Fermion-spin transformation to implement the charge-spin separation. *Phys. Rev. B* **49**, 2368–2384 (1994).
61. Pruschke, T. & Shiba, H. Correlation functions and critical exponents in the one-dimensional anisotropic t-j model. *Phys. Rev. B* **44**, 205–216 (1991).
62. Li, J., Golež, D., Werner, P. & Eckstein, M. Superconducting optical response of photodoped mott insulators. *Mod. Phys. Lett. B* **34**, 2040054 (2020).
63. Lange, F., Lenarčič, Z. & Rosch, A. Time-dependent generalized gibbs ensembles in open quantum systems. *Phys. Rev. B* **97**, 165138 (2018).
64. Golež, D., Eckstein, M. & Werner, P. Dynamics of screening in photodoped mott insulators. *Phys. Rev. B* **92**, 195123 (2015).
65. Kotliar, G. & Ruckenstein, A. E. New functional integral approach to strongly correlated fermi systems: the gutzwiller approximation as a saddle point. *Phys. Rev. Lett.* **57**, 1362–1365 (1986).
66. Ogata, M. & Fukuyama, H. The T-J model for the oxide high-Tc superconductors. *Rep. Prog. Phys.* **71**, 036501 (2008).
67. Corboz, P., Orús, R., Bauer, B. & Vidal, G. Simulation of strongly correlated fermions in two spatial dimensions with fermionic projected entangled-pair states. *Phys. Rev. B* **81**, 165104 (2010).
68. Misawa, T. et al. mvmc² open-source software for many-variable variational monte carlo method. *Computer Phys. Commun.* **235**, 447–462 (2019).
69. Werner, P. & Murakami, Y. Light-induced hidden odd-frequency order in a model for A_3C_{60} . *Phys. Rev. B* **104**, L201101 (2021).
70. Tsuji, N., Nakagawa, M. & Ueda, M. Tachyonic and plasma instabilities of η -pairing states coupled to electromagnetic fields. Preprint at [arXiv:2103.01547](https://arxiv.org/abs/2103.01547) (2021).

Acknowledgements

We thank T. Oka and F. Sekiguchi for their helpful discussions. The calculations have been performed on the Beo05 cluster at the University of Fribourg. This work is supported by Grant-in-Aid for Scientific Research from JSPS, KAKENHI Grant Nos. JP19K23425 (Y.M.), JP20K14412 (Y.M.), JP20H05265 (Y.M.), JP21H05017 (Y.M.), JP21K03412 (S.T.), JST CREST Grant No. JPMJCR1901 (Y.M.), JPMJCR19T3 (Y.M. and S.T.), Slovenian Research Agency (ARRS) Grant No. J1-2455 and P1-0044 (D.G.), and ERC Consolidator Grant No. 724103 (P.W.). A.J.M. is supported in part by Programmable Quantum Materials, an Energy Frontier Research Center funded by the US Department of Energy (DOE), Office of Science, Basic Energy Sciences (BES), under award DE-SC0019443. The Flatiron Institute is a division of the Simons Foundation. T.K. was supported by the JSPS Overseas Research Fellowship.

Author contributions

Y.M., D.G., and P.W. conceived the project. P.W. and A.M. supervised the project. Y.M. made all the numerical simulations. Y.M. and S.T. contributed to the iTEDB code. T.K., Z.S., and the rest of the authors contribute to the discussion and the writing of the manuscript.

Competing interests

The authors declare no competing interests.

Additional information

Supplementary information The online version contains supplementary material available at <https://doi.org/10.1038/s42005-021-00799-7>.

Correspondence and requests for materials should be addressed to Yuta Murakami.

Peer review information *Communications Physics* thanks the anonymous reviewers for their contribution to the peer review of this work.

Reprints and permission information is available at <http://www.nature.com/reprints>

Publisher's note Springer Nature remains neutral with regard to jurisdictional claims in published maps and institutional affiliations.



Open Access This article is licensed under a Creative Commons Attribution 4.0 International License, which permits use, sharing, adaptation, distribution and reproduction in any medium or format, as long as you give appropriate credit to the original author(s) and the source, provide a link to the Creative Commons license, and indicate if changes were made. The images or other third party material in this article are included in the article's Creative Commons license, unless indicated otherwise in a credit line to the material. If material is not included in the article's Creative Commons license and your intended use is not permitted by statutory regulation or exceeds the permitted use, you will need to obtain permission directly from the copyright holder. To view a copy of this license, visit <http://creativecommons.org/licenses/by/4.0/>.

© The Author(s) 2022